InGaAs/InP single-photon detector gated at 1.3 GHz with 1.5 % afterpulsing

Carmelo Scarcella, *Member, IEEE,* Gianluca Boso, *Member, IEEE*, Alessandro Ruggeri, *Student Member, IEEE*, Alberto Tosi, *Member, IEEE*

***Abstract*—We demonstrate a single-photon detector based on InGaAs/InP single-photon avalanche diodes (SPADs) sinusoidal-gated at 1.3 GHz with very low afterpulsing (about 1.5 %), high dynamic range (maximum count rate is 650 Mcount/s), high photon detection efficiency (> 30 % at 1550 nm), low noise (per-gate dark count rate is $2.2 \cdot 10^{-5}$) and low timing jitter (< 70 ps full-width at half maximum). The SPAD is paired with a "dummy" structure that is biased in anti-phase. The sinusoidal gating signals are cancelled by means of a common-cathode configuration and by adjusting the relative amplitude and phase of the signals biasing the two arms. This configuration allows to adjust the gating frequency from 1 GHz to 1.4 GHz and can be operated also in the so-called gate-free mode, with the gate sine-wave unlocked with respect to the light stimulus, resulting in a free-running equivalent operation of the InGaAs/InP SPAD with about 4 % average photon detection efficiency at 1550 nm.**

***Index Terms* — Photodetectors, Single-Photon Avalanche Diodes, photon counting, near-infrared detector, Avalanche Photodiode.**

I. Introduction

SINGLE photon detectors for the near-infrared wavelength range between 1 µm and 1.7 µm are widely used in a growing number of applications, such as quantum cryptography (Quantum Key Distribution, QKD) [1], Optical Time Domain Reflectometry (OTDR) [2], eye-safe laser ranging (Light Detection And Ranging, LIDAR) [3], VLSI circuit characterization based on electroluminescence from hot carriers in MOSFETs [4], singlet oxygen detection for dosimetry in PhotoDynamic Therapy (PDT) [5], time-resolved spectroscopy [6], etc. Most of these applications work at 1550 nm with fiber-based systems and require high count rates (greater than some Mcount/s), high detection efficiency (higher than 30%), low noise (few kcount/s), narrow temporal response (with a full-width at half maximum – FWHM – lower than 200 ps). Others applications need to detect single photons from a wider spectral range, from 1 µm to 1.7 µm, with better temporal response (FWHM < 100 ps) and from a free-space coupled source.

InGaAs/InP Single-Photon Avalanche Diodes (SPADs) [7] [8] are among the best single-photon detectors not only for their good performance, but also for their easier implementation in practical and reliable systems when compared to other solutions, such as cryogenic cooled detectors [9]. The main bottleneck of InGaAs/InP SPADs is the afterpulsing effect, which refers to avalanches triggered by carriers correlated to the previous avalanches. During an avalanche event, some charge carriers are trapped in deep levels traps and are then released, with lifetimes that can be as long as tens or hundreds of microseconds [8], thus triggering new avalanches that increase the detector noise. When InGaAs/InP SPADs are operated with square gates lasting few nanoseconds or longer, long hold-off times (in the order of tens of microseconds) are needed after each avalanche in order to limit afterpulsing, thus eventually restricting the maximum count rate.

Afterpulsing can be reduced either at the device level, by reducing the number of deep level traps, thanks to better fabrication processes, or at the circuit level, by reducing the number of charge carriers flowing during each avalanche pulse. The latter approach is achieved by operating InGaAs/InP SPADs with very narrow gate pulses, lasting few hundreds of picoseconds. In literature there are different fast-gating methods, some based on sub-nanosecond square-wave gate signals [10][11], while others based on gigahertz sine wave gating [12][13][14]. In these approaches, the signal at the output of the SPAD includes a small avalanche pulse (whose amplitude is just few millivolts) and a strong disturbance (whose amplitude is orders of magnitude higher than the avalanche pulse) due to the capacitive feed-through of the gate pulses. Various solutions have been reported in literature, including: i) low-pass filters and/or notch filters that cancel the various harmonics of the gate waveform, but degrade the avalanche signal by affecting its high-frequency components; ii) self-differencing schemes that require wide-bandwidth delay lines and a adding circuit placed where the avalanche signal has to be read out, thus limiting the bandwidth of the read-out circuit; iii) harmonic subtraction

Manuscript received August 1, 2014.

A. Tosi and A. Ruggeri are with the Dipartimento di Elettronica, Informazione e Bioingegneria, Politecnico di Milano, Milano 20133, Italy (e-mail: alberto.tosi@polimi.it; alessandro.ruggeri@polimi.it).

C. Scarcella was with the Dipartimento di Elettronica, Informazione e Bioingegneria, Politecnico di Milano, Milano 20133, Italy. He is now with Tyndall National Institute, University College Cork, Lee Maltings, Cork, Ireland (e-mail: carmelo.scarcella@polimi.it).

G. Boso was with the Dipartimento di Elettronica, Informazione e Bioingegneria, Politecnico di Milano, Milano 20133, Italy. He is now with the Group of Applied Physics, University of Geneva, Geneva 4, CH-1211, Switzerland (e-mail: gianluca.boso@polimi.it).

DOI: 10.1109/JSTQE.2014.2361790

that requires to precisely generate few different harmonics of the gate signal to be subtracted at the read-out node.

However, all the components placed on the read-out path may degrade the avalanche signal due to their limited bandwidth and nonlinear frequency response that results in additional time jitter on the avalanche read-out. Moreover, hardware changes on notch filters and self-differencing circuits are needed to adjust the gate frequency.

The goal of our work is to reduce the avalanche charge while preserving low-jitter temporal response and high photon detection efficiency. Additionally, the gate frequency should be adjustable in a wide range to adapt the detector to various application needs and it should be possible to work in "gate-free mode" [15], with the gate waveform unlocked from the light source. Finally, there should be an actual perspective for an easy development of a stable system that can operate continuously in real settings.

II. High-frequency balanced detector configuration

We present a single-photon detector based on InGaAs/InP SPADs that are sinusoidal-gated at f_{GATE} = 1.3 GHz. A SPAD-dummy balancing technique was previously demonstrated for silicon [16] and InGaAs/InP [17] SPADs operated with long (at least few nanoseconds) square-wave gates and is here exploited as an alternative to standard read-out circuits. The detector balanced configuration derives from what reported in Ref. [18], but for the first time it is applied to a gigahertz sinusoidal-gated system.

In order to demonstrate this approach, we developed the experimental setup shown in Fig. 1. A wide-band balun splits the output of a low-power high-frequency sine-wave generator (V_{SIN}) into two paths, phase shifted by 180°. Each path consists of a chain of RF gain stages that amplify by 33 dB the input signal. The two anti-phase signals are then fed to two single-photon avalanche diodes, both integrated in the same chip but with different breakdown voltages (V_{BD}): the first one will be addressed as "SPAD", while the second one will be addressed as "dummy" and has a breakdown voltage about 10 V higher than the SPAD's one. The difference in the breakdown voltage is due to different p-type diffusion in the "dummy" diode compared to the SPAD. Therefore the "dummy" mimics very well the parasitic capacitances and inductances, but no avalanche is triggered in it since we never apply voltages exceeding its breakdown level (i.e. the maximum gate amplitude is lower than 10 V).

The two diodes are both biased at the SPAD breakdown voltage (i.e. V_{BIAS} ~ 65 V at a temperature of 240 K), the gate signals are applied at the anodes, while the avalanche signal is picked-up from the common cathode node. The SPAD is periodically biased above its breakdown voltage by the gate signal, while the "dummy" is always under its breakdown voltage.

Thanks to the proposed structure, the SPAD gate feed-through is balanced with its own anti-phase copy (propagating through the "dummy" path) at the common cathode node, i.e. the readout node.

An RF low-noise amplifier is AC coupled to the readout node, through the pick-up capacitor C_P = 100 nF. It amplifies the avalanche signal by 20 dB and its output is fed to a fast comparator to extract a digital pulse synchronous with the photon arrival. The comparator includes a monostable to provide a fixed-duration output pulse and to implement a count-off time after each avalanche. During the count-off time, spikes and oscillations generated at the readout node are masked.

In order to reduce the primary dark count rate of the InGaAs/InP SPAD, the detection system is cooled at 240 K: the chip including SPAD and "dummy" diodes is mounted onto a custom front-end board and installed into a vacuum chamber onto a four-stage thermo-electric cooler. The

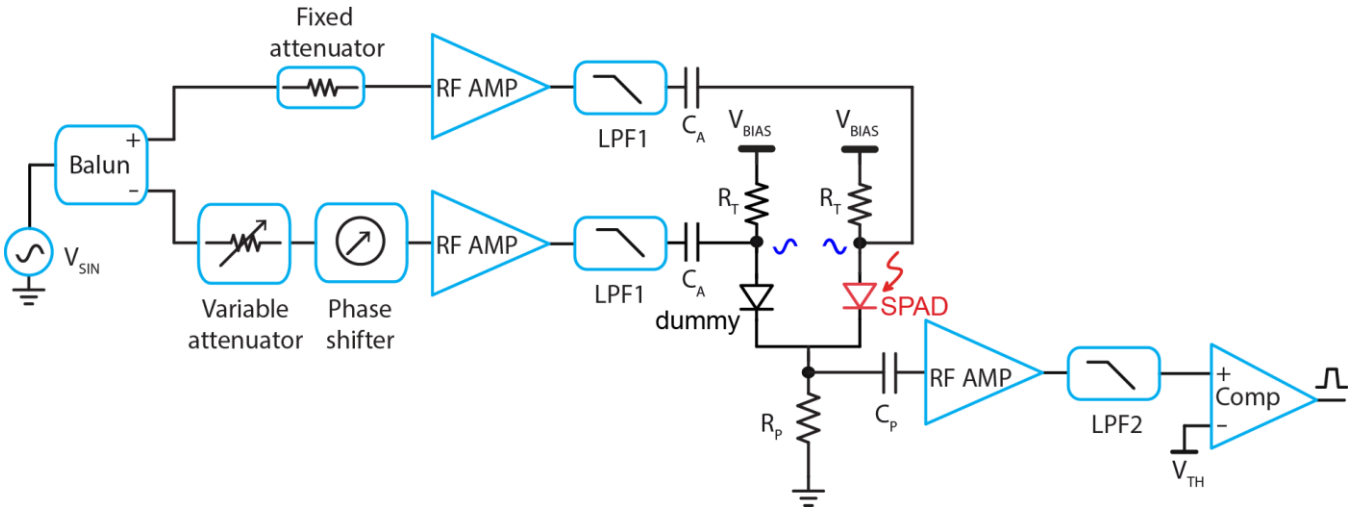

Fig. 1. Block diagram of the experimental setup. By adjusting the amplitude and phase, the capacitive coupling (through SPAD and "dummy") of the gate signal are in anti-phase at the common cathode node for a good rejection. RF AMP: wide-bandwidth amplifier. LPF1 = low-pass filter at 1.45 GHz. LPF2 = low-pass filter at 2.4 GHz. Comp = wide-bandwidth comparator with NIM (Nuclear Instrumentation Module) output. V_{TH} = threshold of the comparator.

detectors are wire-bonded to two RF resistors R_T = 200 Ω (this value was chosen as a trade-off between power dissipation and input return loss of the front-end) and to the resistor R_P = 50 Ω that provides the DC biasing of the device.

The symmetry of the SPAD-dummy approach greatly suppresses the gate feed-through spurious signals, but component tolerances may introduce some residual mismatches. Therefore, in order to achieve a higher suppression factor, the relative phase and amplitude of both sinusoidal gates at f_{GATE} = 1.3 GHz need to be finely adjusted. This is implemented using a RF variable attenuator and a RF variable phase shifter in the "dummy" path. They are both voltage controlled and allow for fine tuning of relative phase and amplitude of the two gates. A 3 dB fixed attenuator in the SPAD path balances the insertion losses of these components in the "dummy" path.

Fig. 2 reports the spectrum of the output node in order to show the suppression of the first harmonic. By introducing the "dummy" path compensation, the first harmonic is attenuated by 60 dB. This differential technique allows for high rejection of the main harmonic component of the gate frequency, but higher order harmonics, mainly generated by nonlinearities of RF amplifiers and SPADs, are still present. These undesired signals are rejected using low-pass filters with two different cut-off frequencies (f_{CO}). A first low-pass filter (LPF1 @ f_{CO1} = 1.45 GHz) is used between the last power amplifier and the front-end board to suppress the harmonics generated by the RF amplifiers. A second low-pass filter (LPF2 @ f_{CO2} = 2.4 GHz) is connected between the output amplifier and the comparator. The cut-off frequency of LPF2 has to be low enough in order to suppress the second harmonic (typically at $2 \cdot f_{GATE}$ = 2.6 GHz in our experimental setup) and sufficiently high to include the whole spectrum of the avalanche pulse, in order to avoid degradation of the photon timing resolution.

In order to estimate the avalanche spectrum, we analyzed with a spectrum analyzer the signal picked up just after C_P in

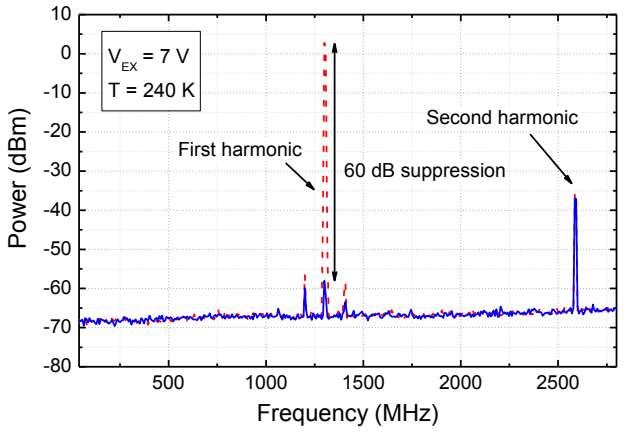

Fig. 2. The spectrum of the output node in two different conditions: the red dashed line is measured without the "dummy" path compensation, while the blue continuous one is after adding the anti-phase signal of the "dummy" path. The resulting rejection of the first harmonic of the gate signal at f_{GATE} = 1.3 GHz is more than 60 dB. The side peaks around the first harmonic are due to a spurious tone at the output of the 1.3 GHz sinusoidal generator.

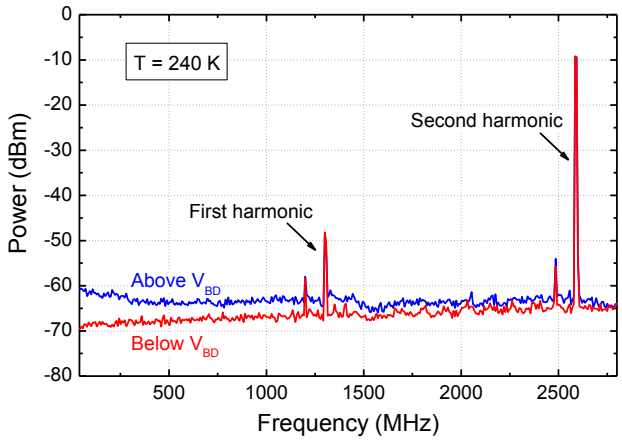

Fig. 3. Spectrum of the signal picked up just after the capacitor C_P, with no filtering of the second harmonic, in two cases: i) with V_{BIAS} equal to the SPAD breakdown voltage (64.5 V); ii) with V_{BIAS} below the SPAD breakdown voltage (54.5 V). In both cases the sinusoidal peak-to-peak amplitude was 14 V, i.e. the same sinusoidal signal used for achieving an excess bias of 7 V. The difference between the two curves is due to the avalanche pulse, since in the blue curve the SPAD is biased above its breakdown level for half of the time.

two cases (see Fig. 3): i) with V_{BIAS} above the SPAD breakdown voltage; ii) with V_{BIAS} below the SPAD breakdown voltage. The difference between the two curves is due to the avalanche pulse contribution. Therefore from Fig. 3 it is possible to infer that the avalanche spectrum extends to at least 2 GHz. Finally, from this trade-off we chose f_{CO2} = 2.4 GHz.

III. Experimental Measurements

The system here described has been characterized with an InGaAs/InP SPAD developed at Politecnico di Milano [7]. The peculiar structure we used consists of an InGaAs/InP SPAD with 25 µm active area diameter coupled on the same die with the "dummy" structure that mimics the electrical response of the detector, but it is insensitive to impinging photons. SPAD and "dummy" diodes have common cathode contact on the chip backside and separate anode contacts on the chip topside. The detector is cooled at 240 K. The SPAD breakdown voltage at this temperature is 64.5 V, while that of the "dummy" structure is about 10 V higher. A sinusoidal voltage at f_{GATE} = 1.3 GHz is AC coupled to the SPAD anode, while its copy, shifted by 180°, is applied to the anode of the "dummy" structure. The DC bias (V_{BIAS}) is equal to the SPAD breakdown voltage.

We experimentally characterized the proposed system in terms of dark count rate, afterpulsing probability, photon detection efficiency, timing resolution and maximum sustainable count rate.

A. *Dark count rate and afterpulsing probability*

The primary dark count rate is basically not affected by the gating technique, but it is due to the intrinsic structure and material quality of the InGaAs/InP SPADs. However, a low threshold has to be used in order to avoid missing small avalanche pulses (both dark counts and photon counts) mainly due to avalanches triggered towards the end of the gate signal.

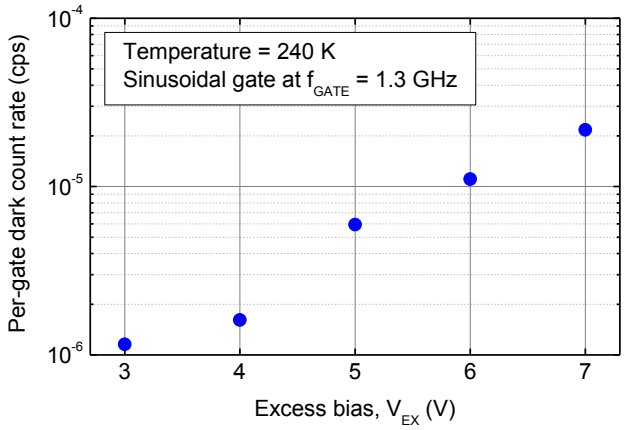

Fig. 4. Dependence of the per-gate dark count rate on the excess bias (i.e. the amplitude of the sinusoidal gate at 1.3 GHz).

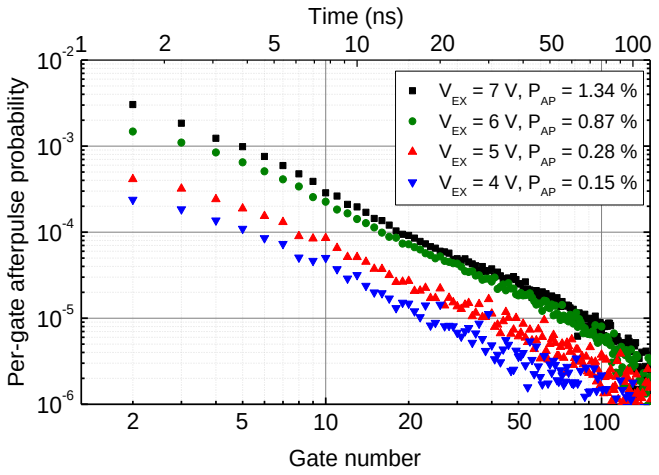

Fig. 5. Per-gate afterpulsing probability as a function of number of gates after the first reference avalanche, at four different excess bias voltages. Scale on top represents the time elapsed from the first reference avalanche. The total afterpulsing probability (P_{AP}) is calculated integrating the per-gate afterpulsing probability.

The measured per-gate dark count rate, with the minimum comparator threshold (i.e. about 20 mV), is about 1×10^{-6} when the excess bias (i.e. the amplitude of the sinusoidal gate) is $V_{EX} = 3$ V, and increases with an exponential dependence up to 2×10^{-5} at $V_{EX} = 7$ V (see Fig. 4).

The afterpulsing probability has been characterized with the Time-Correlated Carrier Counting (TCCC) technique [19]. Fig. 5 shows the per-gate afterpulsing probability at different excess-bias voltages. Afterpulses have been recorded starting from the second gate after the avalanche, since the first one is masked by the count-off time given by the monostable of the fast comparator.

In good agreement with what reported in Ref. [20], experimental data exhibit a power-law dependence over a time scale of about 100 ns. We calculated the total afterpulsing probability by integrating the curves of Fig. 5. The maximum total afterpulsing probability at $V_{EX} = 7$ V is 1.34 %, while it is even below 0.2 % at $V_{EX} = 4$ V. This remarkable result can be easily halved increasing the count-off time to 5 ns (i.e. by skipping 6 gates after the first reference avalanche).

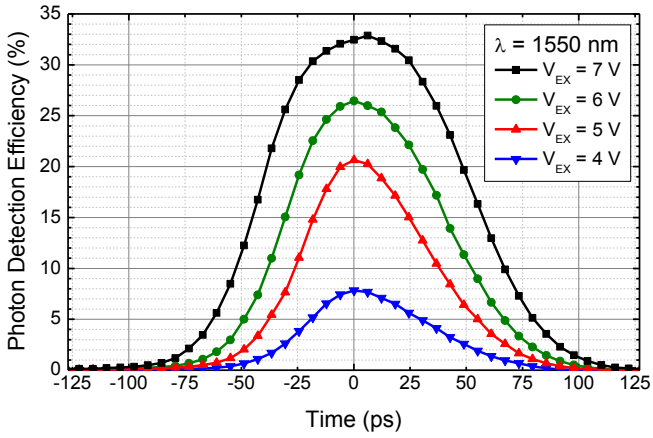

Fig. 6. Photon detection efficiency at λ = 1550 nm within the gate at four different excess bias voltages. The full-width at half maximum of the curves is about 60-100 ps.

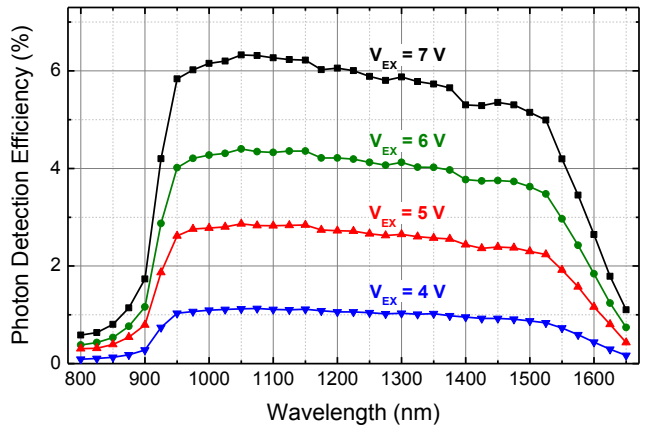

Fig. 7. Average photon detection efficiency of the system measured in the wavelength range from 800 nm to 1650 nm with the sinusoidal gate unlocked from the light source. At λ = 1550 nm, the average PDE exceeds 4% when the excess bias voltage is $V_{EX} = 7$ V.

B. *Photon detection efficiency*

We measured the system Photon Detection Efficiency (PDE) at λ = 1550 nm within the gate at different excess bias voltages by means of a calibrated optical test bench. The measurement setup is based on a broadband light source (quartz lamp), a monochromator and an integrating sphere. The monochromator selects the wavelength and the integrating sphere is used to uniformly illuminate the active area of the detector. The optical power is monitored by a calibrated power meter mounted on a secondary output of the integrating sphere. The optical signal is attenuated down to single-photon level and about 10^6 photons imping on the detector every second,

i.e. about one photon every 1300 gates. The system PDE is the ratio between the number of photons impinging on the detector active area and the output pulses.

We acquired the arrival times of the triggered avalanche pulses by means of a Time-Correlated Single-Photon Counting (TCSPC) board. Fig. 6 shows the time distribution of the triggered avalanches within the gate. The maximum PDE at the center of the gate is more than 30 % at V_{EX} = 7 V. Such value is comparable to what measured when the InGaAs/InP SPAD is operated with square-wave gates lasting at least some nanoseconds. The full-width at half maximum of the distribution is about 100 ps at all the excess bias voltages, thus showing that most of the avalanches are triggered when the gate is around its maximum.

The spectral dependence of the Photon Detection Efficiency (PDE) of the system has been measured using the same calibrated optical test bench, but with a photon counter in place of the TCSPC board. Fig. 7 shows the average PDE of the system in the wavelength range between 800 nm and 1650 nm (with 25 nm steps) at different excess bias voltages. Since the light source is not locked with the sinusoidal gate, the measured value is the average PDE [15]. At V_{EX} = 7 V, the average PDE peaks at about 6 % and is still about 4.2 % at 1550 nm. When the detector is operated with a square-wave gate, the resulting PDE can be almost an order of magnitude higher, but the enabling duty-cycle is usually even below 1% to mitigate afterpulsing (e.g. with 100 ns ON time and 10 µs OFF time, the duty cycle is 1%). This leads to a much lower average PDE that prevents the use of InGaAs/InP SPAD operated in gated mode for measuring CW sources.

C. *Timing jitter*

In order to measure the timing resolution of our system, we employed a picosecond pulsed laser emitting narrow pulses (< 20 ps FWHM) at 1550 nm with repetition frequency of 1 MHz. The response of our system has been measured both with the laser pulses synchronized with the 1.3 GHz gate frequency and with the laser pulses unlocked from the gate waveform, in the so-called "gate-free" mode [15]. For both measurements, the InGaAs/InP SPAD is operated with an excess bias of 7 V and the incoming photon rate is about $6 \cdot 10^5$ photons per second.

During the synchronized measurement, the laser trigger is derived from the 1.3 GHz gate frequency and is properly delayed, through a programmable wideband delay line, in order to center the laser pulse on the peak of the sine-wave modulating signal. In the "gate-free" mode, instead, the laser trigger and the detector gating frequency are completely independent.

Fig. 8 shows the response of the detector biased with V_{EX} = 7 V to a pulsed laser source synchronous with the peak of the gate signal. The timing jitter is very low, being just 65 ps (FWHM). The small peaks are due to dark counts or background photons (i.e. stray light) triggering avalanches in all the gates.

Fig. 9 shows the response of the detector in the "gate-free" regime. The response is slightly broader, being about 88 ps (FWHM), but narrower than what achieved with our previous setup [15] thanks to a lower detection threshold given by a better rejection of the gate waveform. The small "bump" after the main peak is due to afterpulses generated by avalanches not detected in the preceding gate. Since small avalanches (e.g. those generated at the end of the gate) are not sensed by the comparator, their afterpulses cannot be masked by the count-off time and are accumulated in the next gate, thus forming the residual "bump" few orders of magnitude lower than the main peak. This phenomenon is strongly attenuated with respect to our previous setup [15] thanks to better gate feed-through rejection, resulting in a lower avalanche detection threshold.

D. *Saturated count rate*

Given the very low afterpulsing (< 1.5%) even with a short count-off time, we characterize the linearity of the response to a light stimulus. With just 1.5 ns, only a single gate after each avalanche detection is skipped.

Fig. 10 shows the dependence of the output count rate on a constant increase in the illuminating photon flux until saturation is reached. The experimental points (dots) are in good agreement with the theoretical behavior of a single-photon detector with a count-off time of 1.54 ns (blue line), corresponding to a maximum count rate of 650 Mcps.

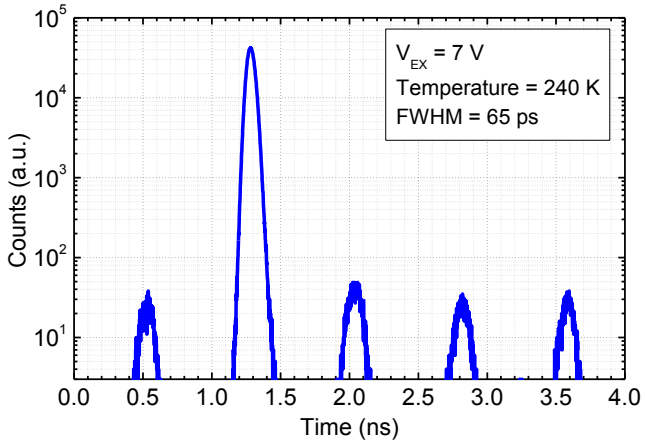

Fig. 8. Temporal response of the InGaAs/InP SPAD system sinusoidally gated at 1.3 GHz, with the laser source synchronous with the gate waveform.

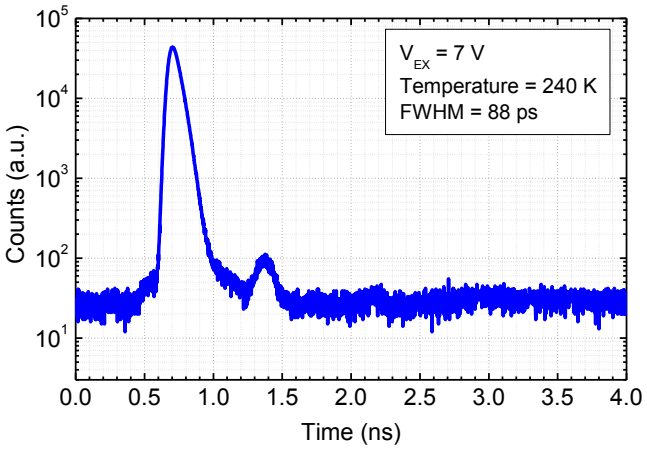

Fig. 9. Temporal response of the InGaAs/InP SPAD system sinusoidally gated at 1.3 GHz, with the laser source not locked with the gate waveform.

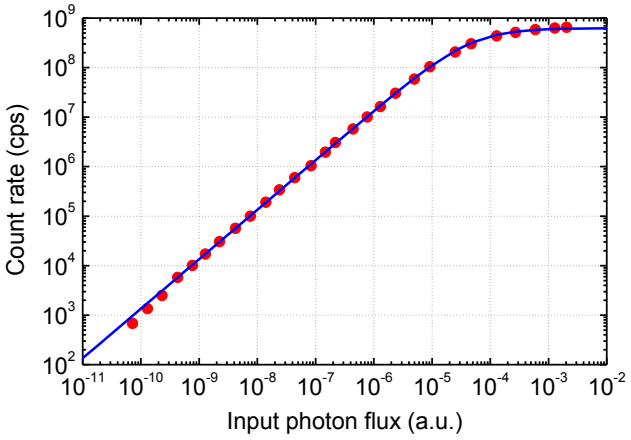

Fig. 10. Dependence of the count rate on the input photon flux. The linearity is very good over many decades. The maximum saturated count rate is about 650 Mcps.

IV. Conclusion

We presented a photon-counting system based on InGaAs/InP SPADs sinusoidal-gated at 1.3 GHz with very low afterpulsing (about 1.5 %), high dynamic range (maximum count rate is 650 Mcount/s), high photon detection efficiency (> 30 % at 1550 nm), low noise (per-gate dark count rate is $2.2 \cdot 10^{-5}$) and low timing jitter (< 70 ps). The joint use of a balanced detector configuration and proper low pass filters guarantees to achieve a good suppression of the gate signal coupling without affecting the avalanche spectrum, thus allowing for detecting avalanches with no distortion and with low threshold.

Besides the good performances, this configuration is advantageous because: it allows to adjust the gating frequency in a wide range, from 1 GHz to 1.4 GHz; it can be operated also in the so-called "gate-free" mode, with the gate sinusoid unlocked with respect to the light stimulus; by adding a feedback loop, the attenuation and phase shift can be automatically adjusted in order to optimize the gate feed-through suppression and have a stable system that can operate continuously in real settings.

Acknowledgment

The authors wish to thank Franco Zappa, Fabio Acerbi, Mirko Sanzaro, Niccolò Calandri and Andrea Grande for their useful discussions and contributions.

References

[1] N. Gisin and R. Thew, "Quantum communication," Nature Photonics, vol. 1, no. 3, pp. 165–171, Mar. 2007.

[2] P. Eraerds, M. Legre, J. Zhang, H. Zbinden, and N. Gisin, "Photon Counting OTDR: Advantages and Limitations," J. Light. Technol., vol. 28, no. 6, pp. 952–964, Mar. 2010.

[3] Y. Liang, J. Huang, M. Ren, B. Feng, X. Chen, E. Wu, G. Wu, and H. Zeng, "1550-nm time-of-flight ranging system employing laser with multiple repetition rates for reducing the range ambiguity," Optics Express vol 22, no. 4, p. 4662, Feb. 2014.

[4] F. Stellari, P. Song, and A. J. Weger, "Single Photon Detectors for Ultra Low Voltage Time-Resolved Emission Measurements," IEEE J. Quantum Electron., vol. 47, no. 6, pp. 841–848, Jun. 2011.

[5] N. R. Gemmell, A. McCarthy, B. Liu, M. G. Tanner, S. D. Dorenbos, V. Zwiller, M. S. Patterson, G. S. Buller, B. C. Wilson, and R. H. Hadfield, "Singlet oxygen luminescence detection with a fiber-coupled superconducting nanowire single-photon detector," Optics Express, vol. 21, no. 4, p. 5005, Feb. 2013.

[6] I. Bargigia, A. Tosi, A. Bahgat Shehata, A. Della Frera, A. Farina, A. Bassi, P. Taroni, A. Dalla Mora, F. Zappa, R. Cubeddu, and A. Pifferi, "Time-resolved diffuse optical spectroscopy up to 1700 nm by means of a time-gated InGaAs/InP single-photon avalanche diode.," Appl. Spectrosc., vol. 66, no. 8, pp. 944–50, Aug. 2012.

[7] A. Tosi, F. Acerbi, M. Anti, and F. Zappa, "InGaAs/InP Single-Photon Avalanche Diode With Reduced Afterpulsing and Sharp Timing Response With 30 ps Tail," IEEE J. Quantum Electron., vol. 48, no. 9, pp. 1227–1232, Sep. 2012.

[8] M. A. Itzler, X. Jiang, M. Entwistle, K. Slomkowski, A. Tosi, F. Acerbi, F. Zappa, and S. Cova, "Advances in InGaAsP-based avalanche diode single photon detectors," J. Mod. Opt., vol. 58, no. 3–4, pp. 174–200, Feb. 2011.

[9] G. N. Gol'tsman, O. Okunev, G. Chulkova, A. Lipatov, A. Semenov, K. Smirnov, B. Voronov, A. Dzardanov, C. Williams, and R. Sobolewski, "Picosecond superconducting single-photon optical detector," Applied Physics Letters, vol. 79, no. 6, pp. 705–707, 2001.

[10] A. Restelli, J. C. Bienfang, and A. L. Migdall, "Time-domain measurements of afterpulsing in InGaAs/InP SPAD gated with sub-nanosecond pulses," Journal of Modern Optics, vol. 59, no. 17, pp. 1465–1471, May 2012.

[11] K. A. Patel, J. F. Dynes, A. W. Sharpe, Z. L. Yuan, R. V. Penty, and A. J. Shields, "Gigacount/second photon detection with InGaAs avalanche photodiodes," Electronics Letters, vol. 48, no. 2, p. 111, 2012.

[12] N. Namekata, S. Adachi, and S. Inoue, "Ultra-Low-Noise Sinusoidally Gated Avalanche Photodiode for High-Speed Single-Photon Detection at Telecommunication Wavelengths," IEEE Photonics Technology Letters, vol. 22, no. 8, pp. 529–531, Apr. 2010.

[13] J. Zhang, P. Eraerds, N. Walenta, C. Barreiro, R. Thew, and H. Zbinden, "2.23 GHz gating InGaAs/InP single-photon avalanche diode for quantum key distribution," in Proc. SPIE 7681, Advanced Photon Counting Techniques IV, 2010, p. 76810Z–76810Z–8.

[14] Y. Liang, E. Wu, X. Chen, M. Ren, Y. Jian, G. Wu, and H. Zeng, "Low-Timing-Jitter Single-Photon Detection Using 1-GHz Sinusoidally Gated InGaAs/InP Avalanche Photodiode," IEEE Photonics Technology Letters, vol. 23, no. 13, pp. 887–889, Jul. 2011.

[15] A. Tosi, C. Scarcella, G. Boso, and F. Acerbi, "Gate-Free InGaAs/InP Single-Photon Detector Working at Up to 100 Mcount/s," IEEE Photonics J., vol. 5, no. 4, pp. 6801308–6801308, Aug. 2013.

[16] G. Boso, A. Dalla Mora, A. Della Frera, and A. Tosi, "Fast-gating of single-photon avalanche diodes with 200ps transitions and 30ps timing jitter," Sensors Actuators A Phys., vol. 191, pp. 61–67, Mar. 2013

[17] A. Tosi, A. Della Frera, A. Bahgat Shehata, and C. Scarcella, "Fully programmable single-photon detection module for InGaAs/InP single-photon avalanche diodes with clean and sub-nanosecond gating transitions," The Review of scientific instruments, vol. 83, no. 1, p. 013104, Jan. 2012.

[18] Z. Lu, W. Sun, Q. Zhou, J. C. Campbell, X. Jiang, and M. A. Itzler, "Improved sinusoidal gating with balanced InGaAs/InP Single Photon Avalanche Diodes.," Opt. Express, vol. 21, no. 14, pp. 16716–21, Jul. 2013.

[19] A. C. Giudice, M. Ghioni, S. Cova, and F. Zappa, "A process and deep level evaluation tool: afterpulsing in avalanche junctions," in European Solid-State Device Research, 2003. ESSDERC '03. 33rd Conference on, 2003, pp. 347–350.

[20] M. A. Itzler, X. Jiang, and M. Entwistle, "Power law temporal dependence of InGaAs/InP SPAD afterpulsing," J. Mod. Opt., vol. 59, no. 17, pp. 1472–1480, Oct. 2012.

Alberto Tosi was born in Borgomanero, Italy, in 1975. He received the Master degree in electronics engineering and the Ph.D. degree in information technology engineering from the Politecnico di Milano, Milan, Italy, in 2001 and 2005, respectively. He has been an Assistant Professor of Electronics at Politecnico di Milano since 2006. In 2004, he was a student with the IBM T.J. Watson Research Center, Yorktown Heights, NY, working on optical testing of CMOS circuits. Currently, he works on silicon and InGaAs/InP single-photon avalanche diodes (SPADs). He is involved in research on arrays of silicon SPADs for 2D and 3D applications and on time-correlated single-photon counting electronics.

Carmelo Scarcella was born in Milazzo, Italy, in 1985. He was awarded the Master degree in electronics engineering and the Ph.D. in information technology engineering at Politecnico di Milano, Milano, Italy, in 2010 and 2014, respectively. He is currently working with the Integrated Photonics Group at Tyndall National Institute, Cork, Ireland. His research activity focuses on single-mode optical coupling for photonics technologies and high-speed packaging techniques.

Alessandro Ruggeri was born in Alzano Lombardo, Italy, in 1987. He graduated in Electronics Engineering in 2012 at Politecnico di Milano (Italy), where he is now a Ph.D. student in Information Technology. During the summer of 2014 he was with the IBM T.J. Watson Research Center, Yorktown Heights, NY, working on optical testing of ULSI circuits. His main research interest regards the development of electronics for near-infrared single photon avalanche diodes for biomedical and communications applications.

Gianluca Boso was born in Tione di Trento, Italy, in 1985. He was awarded the Master degree in electronics engineering and the Ph.D. in information technology engineering from Politecnico di Milano, Milano, Italy, in 2010 and 2014 respectively. He is currently working with the Group of Applied Physics at the University of Geneva, Geneva, Switzerland. His research activity focuses on the development of single-photon detectors for quantum communication and biomedical applications.